Mixed Iridium-Gold Hydrides as Model Compounds for Elucidating the Interconversion between Classical and Nonclassical Polyhydrides

Claudio Bianchini,*,† Andrea Meli,† Maurizio Peruzzini,† Alberto Vacca,† Francesco Vizza,† and Alberto Albinati‡

Istituto per lo Studio della Stereochimica ed Energetica dei Composti di Coordinazione, CNR, Via Jacopo Nardi 39, 50132 Firenze, Italy, and Istituto Chimico Farmaceutico e Tossicologico dell'Università di Milano, Viale Abruzzi 41, Milano, Italy

Received January 7, 1992

The reaction of $[(triphos)Ir(H)(C_2H_4)]$ (**1**) or $[(triphos)Ir(H)_2(C_2H_5)]$ (**2**) with $[Au(THF)(PPh_3)]PF_6$ under ethylene produces the monogold adduct $[(triphos)Ir(H)(C_2H_4)\{Au(PPh_3)\}]PF_6$ (**3**) which exhibits a terminal hydride ligand in the solid state, but contains a bridging hydride in solution [triphos = $CH_3C(CH_2PPh_2)_3$]. Addition of 1 equiv of $[AuCl(PPh_3)]$ to **3** yields the iridium-digold adduct $[(triphos)(Cl)Ir(\mu\text{-}H)\{Au_2(PPh_3)_2\}]PF_6$ (**4**). Complex **4** and its arsino analogue $[(triphos)(Cl)Ir(\mu\text{-}H)\{Au_2(AsPh_3)_2\}]PF_6$ (**5**) can be prepared straightforwardly by reacting **1** or **2** with 2 equiv of $[AuCl(EPh_3)]$ (E = P, As) in the presence of NH_4PF_6. The structure of **4** has been determined by X-ray diffraction. Crystals are triclinic, space group $P\bar{1}$ with a = 14.317 (6) Å, b = 17.626 (4) Å, c = 17.791 (2) Å, α = 90.82 (1)°, β = 110.41 (2)°, γ = 112.31 (2)°, V = 3836 (4) Å^3, and Z = 2. The iridium center is coordinated in a distorted octahedral environment by the triphos ligand, a chlorine atom, and two $Au(PPh_3)$ units with the two gold atoms linked to each other. A crystallographically located hydride ligand bridges one of the two Ir-Au edges in the triangular $IrAu_2$ moiety. All of the mixed iridium-gold complexes are fluxional in solution. The fluxional processes have been studied by variable-temperature $^{31}P\{^1H\}$ NMR and ^1H NMR spectroscopy.

Introduction

It is not unusual that a metal complex exhibits different structures on going from the solid state to solution. In most instances, such dichotomies can be discriminated unambiguously by means of spectroscopic and X-ray techniques. However, when polyhydridometal complexes are involved, the question is much more difficult to address due to the uncertainty in locating hydrogen atoms by X-ray diffraction as well as the easiness with which hydrogen atoms exchange their positions or move over complex frameworks.[1-7]

Several examples of different solid-state/solution structures are originated by classical (solid state) ↔ nonclassical (solution) rearrangements of hydride ligands, including cases in which (i) two terminal hydrides couple to give an η^2-H_2 ligand[5] and (ii) a terminal hydride intramolecularly may interact with a dihydrogen ligand to form an η^3-trihydrogen complex in either a transition state or an intermediate.[8-11]

In light of the isolobal relationship between "$Au(EPh_3)$" (E = P, As) and "H" moieties,[12] we started a research program directed to the synthesis of mixed metal-gold hydrides and polyhydrides to see whether the substitution of $Au(EPh_3)$ for H may help in elucidating possible solid-state/solution structural changes or ambiguous fluxional processes of related polyhydridometal complexes. Thus, we hope that the gold atoms, easily located by X-ray diffraction, while mimicking the H ligands, will give valuable information in the assessment of solid-state and solution stereochemistries via the NMR values of the coupling constants associated with the PPh_3 group bonded to gold.[13]

In this paper we report the synthesis and characterization of the iridium-gold hydrides $[(triphos)Ir(H)(C_2H_4)\{Au(PPh_3)\}]PF_6$ (**3**), $[(triphos)(Cl)Ir(\mu\text{-}H)\{Au_2(PPh_3)_2\}]PF_6$ (**4**), and $[(triphos)(Cl)Ir(\mu\text{-}H)\{Au_2(AsPh_3)_2\}]PF_6$ (**5**). From a comparison of the solid-state/solution structures of **3**, we have been able to prove a case of terminal-bridging hydride rearrangement, while the iridium-digold complexes **4** and **5** constitute model compounds for designing an η^3-H_3 complex. However, we acknowledge that there is no evidence of either the dihydrogen form of $[(triphos)Ir(H)_2(C_2H_4)]BPh_4$ or a trihydrogen complex of the formula $[(triphos)Ir(Cl)(H_3)]^+$.[14]

Experimental Section

General Data. Reagent grade chemicals were used in the preparation of the complexes. Tetrahydrofuran (THF) and dichloromethane were purified by distillation over $LiAlH_4$ and P_2O_5 under nitrogen just prior

† ISSECC, CNR.
‡ Università di Milano.

(1) Kubas, G. J. *Acc. Chem. Res.* **1988**, *21*, 120.
(2) Crabtree, R. H.; Hamilton, D. G. *Adv. Organomet. Chem.* **1988**, *28*, 299.
(3) Crabtree, R. H. *Acc. Chem. Res.* **1990**, *23*, 95.
(4) Khalsa, G. R. K.; Kubas, G. J.; Unkefer, C. J.; Van der Sluys, L. S.; Kubat-Martin, K. A. *J. Am. Chem. Soc.* **1990**, *112*, 3855.
(5) Chinn, M. S.; Heinekey, D. M. *J. Am. Chem. Soc.* **1990**, *112*, 5166.
(6) Paciello, R. A.; Manriquez, J. A.; Bercaw, J. E. *Organometallics* **1990**, *9*, 260.
(7) Arliguie, T.; Chaudret, B. *J. Chem. Soc., Chem. Commun.* **1989**, 155.
(8) Luo, X.-L.; Crabtree, R. H. *J. Am. Chem. Soc.* **1990**, *112*, 6912.
(9) (a) Bianchini, C.; Peruzzini, M.; Zanobini, F. *J. Organomet. Chem.* **1988**, *354*, C19.
(10) Bianchini, C.; Peruzzini, M.; Polo, A.; Vacca, A.; Zanobini, F. *Gazz. Chim. Ital.* **1991**, *121*, 543.
(11) Bianchini, C.; Perez, P. J.; Peruzzini, M.; Vacca, A.; Zanobini, F. *Inorg. Chem.* **1991**, *30*, 279.
(12) (a) Hoffmann, R. *Angew. Chem., Int. Ed. Engl.* **1982**, *21*, 711. (b) Stone, F. G. A. *Angew. Chem., Int. Ed. Engl.* **1984**, *23*, 89. (c) Lauher, J. W.; Wald, K. *J. Am. Chem. Soc.* **1981**, *103*, 7648. (d) Housecroft, C. E.; Rheingold, A. L. *Organometallics* **1987**, *6*, 1332. (e) Bateman, L. W.; Green, M.; Mead, K. A.; Mills, R. M.; Salter, I. D.; Stone, R. F. G.; Woodward, P. *J. Chem. Soc., Dalton Trans.* **1983**, 2599. (f) Bianchini, C.; Peruzzini, M.; Zanobini, F. *J. Organomet. Chem.* **1990**, *390*, C16. (g) Bruce, M. I.; Corbin, P. E.; Humphrey, P. A.; Koutsantonis, G. A.; Liddell, M. J.; Tiekink, E. R. T. *J. Chem. Soc., Chem. Commun.* **1990**, 674.
(13) Mueting, A. M.; Bos, W.; Alexander, B. D.; Boyle, P. D.; Casalnovo, J. A.; Balaban, S.; Ito, L. N.; Johnson, S. M.; Pignolet, L. H. *New J. Chem.* **1988**, *12*, 505.
(14) Barbaro, P.; Bianchini, C.; Meli, A.; Peruzzini, M.; Vacca, A.; Vizza, F. *Organometallics* **1991**, *10*, 2227.

0020-1669/92/1331-3841$03.00/0

Scheme I

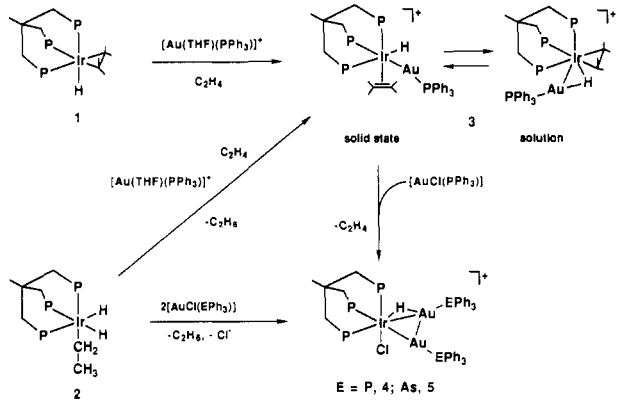

to use, respectively. Deuterated solvents for NMR measurements (Janssen and Aldrich) were dried over molecular sieves. Literature methods were used for the preparation of [(triphos)Ir(H)(C_2H_4)] (**1**),[14] [(triphos)Ir(H)$_2$(C_2H_5)] (**2**),[14] [AuCl(PPh_3)],[15] and [AuCl($AsPh_3$)].[16] Infrared spectra were recorded on a Perkin-Elmer 1600 Series FTIR spectrophotometer using samples mulled in Nujol between KBr plates. NMR spectra were recorded on Varian VXR 300 or Bruker AC 200P instruments operating at 299.94 and 200.13 MHz (^{1}H) and at 121.42 and 81.01 MHz (^{31}P), respectively. The $^{13}C\{^1H\}$ NMR spectra were collected on the Bruker spectrometer at 50.32 MHz. Peak positions are relative to tetramethylsilane as an external reference (^{1}H and $^{13}C\{^1H\}$) or to external 85% H_3PO_4 ($^{31}P\{^1H\}$) with downfield values reported as positive. Proton NMR spectra with selective decoupling of the ^{31}P resonances were recorded on the Bruker AC 200P instrument equipped with a 5-mm inverse probe and a BFX-5 Bruker amplifier device. The spin–lattice relaxation times (T_1) were measured with the inversion-recovery sequence at 299.94 MHz (CD_2Cl_2, 22 °C).

The computer simulation of NMR spectra was carried out with a locally developed package containing the programs LAOCN3[17] and DAVINS,[18] running on a Compaq Deskpro 386/25 personal computer. The initial choices of shifts and coupling constants were refined by iterative least-squares calculations using the experimental digitized spectrum. The final parameters gave a satisfactory fit between experimental and calculated spectra, the agreement factor R being less than 2% in all cases. The line shape analysis of the variable-temperature NMR spectra was accomplished by means of the DNMR3 program[19] adapted for the Compaq computer. Errors in the calculated rate constants were estimated by varying the rate constant around the best-fit value until an observable difference between simulated and experimental spectra, both displayed on the graphical terminal, could be detected. These errors proved to be 5% or less.

Conductivities were measured with an Orion Model 990101 conductance cell connected to a Model 101 conductivity meter. The conductivity data were obtained at sample concentrations of ca. 1×10^{-3} M in nitroethane solutions at room temperature (22 °C).

Analysis of the gaseous products of the reactions was carried out on a Shimadzu GC-8A gas chromatograph fitted with a thermal conductivity detector and with a 10-ft 100/120 Carbosieve-SII stainless-steel column (Supelco Inc.).

Synthesis of the Complexes. All reactions and manipulations were routinely performed under nitrogen, unless otherwise stated, by using Schlenk-tube techniques. The solid complexes were collected on sintered-glass frits and washed with ethanol and petroleum ether (bp 40–70 °C) before being dried under a stream of nitrogen.

The reactions described in this paper are summarized in Scheme I. Selected ^{1}H and $^{13}P\{^1H\}$ NMR spectral data for the complexes are reported in Table I. Significant IR absorptions and $^{13}C\{^1H\}$ NMR data are given in this section or in the rest of the text.

Preparation of [(triphos)Ir(H)(C_2H_4){Au(PPh_3)}]PF_6 (3). Method A. To a THF solution (50 mL) of [(triphos)Ir(H)(C_2H_4)] (**1**) (0.60 g, 0.71 mmol) under a steady stream of ethylene was added a slight excess of [Au(THF)(PPh_3)]PF_6 prepared in situ from [AuCl(PPh_3)] (0.37 g, 0.75 mmol) and $TlPF_6$ (0.27 g, 0.77 mmol) in THF (30 mL). Stirring the solution for 15 min produced a pale yellow color. Addition of an ethanol/*n*-heptane mixture (2:1 v/v, 80 mL) and concentration under a brisk current of ethylene yielded pale yellow crystals of **3**, yield 70%.

Method B. Complex **3** can be obtained in similar yield by treating under ethylene a THF solution (60 mL) of [(triphos)Ir(H)$_2$(C_2H_5)] (**2**) (0.60 g, 071 mmol) with an equivalent amount of [Au(THF)(PPh_3)]PF_6 prepared as above. Workup similar to that used in method A afforded **3**. Λ_M = 79 Ω^{-1} cm^2 mol^{-1}. IR: ν(Ir–H) 2047 cm^{-1} (m). $^{13}C\{^1H\}$ NMR (CD_2Cl_2, 22 °C): δ 42.46 (q, ^2J(CP) = 6.0 Hz, CH_3C), δ 39.96 (q, ^3J(CP) = 10.1 Hz, CH_3C), δ 34.62 (br m, CH_2P), δ 19.85 (br m, C_2H_4). Anal. Calcd for $C_{61}H_{59}AuF_6IrP_5$: C, 50.52; H, 4.10; Ir, 13.25. Found: C, 50.19; H, 4.02; Ir, 13.12.

Preparation of [(triphos)Ir(D)(C_2H_4){Au(PPh_3)}]PF_6 (3-d_1). The monodeuterated complex **3**-d_1 was prepared by substituting **1**-d_1 and C_2H_5OD for **1** and C_2H_5OH in the above method A.

Preparation of [(triphos)(Cl)Ir(μ-H){Au$_2$(PPh_3)$_2$}]PF_6 (4). Method A. A 1-equiv portion of solid [AuCl(PPh_3)] (0.17 g, 0.34 mmol) was added with stirring to a THF solution (50 mL) of **3** (0.50 g, 0.34 mmol) to produce a bright yellow solution that separated lemon yellow crystals of **4** after addition of ethanol and slow concentration under nitrogen; yield 85%.

Method B. A double proportion of solid [AuCl(PPh_3)] (1.20 g, 2.43 mmol) was added portionwise to a stirred THF (100 mL) solution of **1** (1.0 g, 1.18 mmol). Solid NH_4PF_6 (0.20 g, 1.19 mmol) was then added. The mixture was stirred for a further 20 min (during which time the solution became cloudy), and ethanol (100 mL) was added. Slow evaporation of the solvent gave **4** in 70% yield.

Method C. Compound **4** can be prepared in a better yield (≥80%) by substituting **2** (1.0 g, 1.18 mmol) for **1** in procedure B. Λ_M = 72 Ω^{-1} cm^2 mol^{-1}. IR: ν(Ir–H) 1813 cm^{-1} (w br). Anal. Calcd for $C_{77}H_{70}Au_2ClF_6IrP_6$: C, 48.25; H, 3.68; Cl, 1.85; Ir, 10.03. Found: C, 48.10; H, 3.63; Cl, 1.74; Ir, 9.88.

Preparation of [(triphos)(Cl)Ir(μ-H){Au$_2$($AsPh_3$)$_2$}]PF_6 (5). Compound **5**, which contains an $AsPh_3$ ligand coordinated to each gold atom, was prepared as lemon yellow crystals as described above for **4** by using [AuCl($AsPh_3$)] in place of [AuCl(PPh_3)] (80% yield). Λ_M = 70 Ω^{-1} cm^2 mol^{-1}. IR: ν(Ir–H) 1813 cm^{-1} (w br). Anal. Calcd for $C_{77}H_{70}As_2Au_2ClF_6IrP_4$: C, 46.13; H, 3.52; Cl, 1.77; Ir, 9.59. Found: C, 45.98; H, 3.44; Cl, 1.64; Ir, 9.47.

X-ray Diffraction Study. Crystals suitable for X-ray diffraction of compound **4** were obtained by slow crystallization from a THF/ethanol mixture, which gave **4**·C_4H_8O, and are air stable.

A prismatic lemon yellow crystal was mounted on a glass fiber at a random orientation on an Enraf-Nonius CAD4 diffractometer for the unit cell and space group determination and for the data collection. Unit cell dimensions were obtained by a least-squares fit of the 2θ values of 25, high-order reflections [9.6° < θ < 18.2°] using the CAD4 centering routines. Selected crystallographic and other relevant data are listed in Table II; an extended list of structural and data collection parameters is given in the supplementary material (Table SI).

Data were measured with variable scan speed to ensure constant statistical precision on the collected intensities. Three standard reflections ($\bar{1}\,\bar{7}\,1$, $1\,7\,\bar{3}$, $1\,7\,\bar{1}$) were used to check the stability of the crystal and of the experimental conditions and measured every hour, while the orientation of the crystal was checked by measuring the three reflections ($1\,7\,\bar{1}$, $\bar{1}\,\bar{6}\,6$, $\bar{3}\,\bar{3}\,\bar{9}$) every 300 reflections. Data have been corrected for Lorentz and polarization factors and for decay, using the data reduction programs of the CAD4-SDP package.[20] An empirical absorption correction was applied by using azimuthal (Ψ) scans of the three "high-χ" angle reflections (χ > 85.7°; 13.6° < θ < 17.1°).

The standard deviations on intensities were calculated in term of statistics alone, while those on F_o were calculated as reported in Table II. Intensities were considered as observed if $|F_o^2| > 2.5\sigma|F^2|$, and used for the solution and refinement of the structure. A F_o = 0.0 was given to those reflections having negative net intensities.

The structure was solved by a combination of Patterson and Fourier methods and refined by full-matrix least-squares[21] analysis (the function

(15) Bruce, M. I.; Nicholson, B. K.; Bin Shawkataly, O. *Inorg. Synth.* **1989**, *26*, 325.
(16) (a) McAuliffe, C. A.; Parish, R. V.; Randall, P. D. *J. Chem. Soc., Dalton Trans.* **1979**, 1730.
(17) Castellano, S.; Bothner-By, A. A. *J. Chem. Phys.* **1964**, *41*, 3863.
(18) (a) Stephenson, D. S.; Binsch, G. A. *J. Magn. Reson.* **1980**, *37*, 395. (b) Stephenson, D. S.; Binsch, G. A. *J. Magn. Reson.* **1980**, *37*, 409.
(19) Kleier, D. A.; Binsch, G. A. *Computer Program for the Calculation of Complex Exchange-Broadened NMR Spectra*; QCPE Program No. 165.
(20) *Enraf-Nonius Structure Determination Package SDP*; Enraf-Nonius; Delft, The Netherlands.
(21) *CAD4 V5 User's Manual*; Enraf-Nonius: Delft, The Netherlands, 1988.

Table I. Selected NMR Spectral Data for the Complexes

		$^{31}P\{^1H\}$[a]			^1H[b]		
compd	temp, °C	pattern	chem shift[d]	coupling const[e]	chem shift[f] (multiplicity)	assignt (intensity)	coupling const[e]
3	20	A_3B	δ_A −13.02	$J(P_AP_B)$ = 25.0	−10.37 (dq)	Ir*H*Au (1 H)	$J(HP_A)$ = 26.5
			δ_B 48.59				$J(HP_B)$ = 43.2
					2.28 (br)	C_2H_4 (4 H)	
	−80	AB_2C	δ_A −8.80	$J(P_AP_C)$ = 49.6	−9.38 (ddt)	Ir*H*Au (1 H)	$J(HP_A)$ = 79.9
			δ_B −14.99	$J(P_AP_B)$ = 26.9			$J(HP_C)$ = 52.6
			δ_C 48.76	$J(P_BP_C)$ = 20.0			$J(HP_B) \leq 2$
					3.99 (br)	C_2H_4 (2 H)	
					0.99 (br)	C_2H_4 (2 H)	
4	20	ABB′CC′[c]	δ_A −12.54	$J(P_AP_C)$ = 5.8	−2.78 (ttd)	Ir*H*Au (1 H)	$J(HP_A)$ = 10.5
			δ_B −6.99	$J(P_AP_B)$ = 15.9			$J(HP_C)$ = 40.8
			δ_C 44.72	$J(P_BP_C)$[g]			$J(HP_B)$ = 15.8
	−92	ABCDE[h]	δ_A −12.48	$J(P_AP_B)$ = 14.1	−2.60 (br dd)	Ir*H*Au (1 H)	$J(HP_B)$ = 87.5
			δ_B −11.74	$J(P_AP_C)$ = 19.4			$J(HP_E)$ = 40.0
			δ_C −0.59	$J(P_AP_D)$ = 2.4			
			δ_D 46.07	$J(P_AP_E)$ = −10.3			
			δ_E 43.67	$J(P_BP_C)$ = 20.6			
				$J(P_BP_D)$ = 50.4			
				$J(P_BP_E)$ = 122.9			
				$J(P_CP_D)$ = 36.3			
				$J(P_CP_E)$ = 11.2			
				$J(P_DP_E)$ = 11.9			
5[i]	75	AB_2	δ_A −9.57	$J(P_AP_B)$ = 16.0	−3.07 (td)	Ir*H*Au (1 H)	$J(HP_A)$ = 41.5
			δ_B −6.92				$J(HP_B)$ = 10.2
	−60	ABC	δ_A −13.81	$J(P_AP_B)$ = 12.8	−2.75 (ddd)	Ir*H*Au (1 H)	$J(HP_A)$ = −9.0
			δ_B −0.67	$J(P_AP_C)$ = 19.5			$J(HP_B)$ = 83.9
			δ_C −16.27	$J(P_BP_C)$ = 19.7			$J(HP_C) \leq 0.8$[j]

[a] All the proton-decoupled ^{31}P NMR spectra were recorded at 121.42 or 81.01 MHz in CD_2Cl_2 unless otherwise stated. All the ^{31}P NMR spectra exhibit the septet due to the PF_6 counteranion [δ −145.47, septet, $^1J(PF)$ = 707.5 Hz]. [b] All ^1H NMR spectra were recorded at 299.945 or 200.131 MHz in CD_2Cl_2 unless otherwise stated. The resonances due to the hydrogen atoms of the triphos ligand and of the gold-bonded PPh_3 or $AsPh_3$ ligands are not reported. [c] The letters A, B, and B′ refer to the triphos phosphorus atoms, whereas C and C′ denote the P atoms of the triphenylphosphine ligands. [d] In parts per million from external 85% H_3PO_4; downfield values are assumed as positive. [e] Coupling constants (J) are in hertz. [f] In parts per million from external tetramethylsilane. Key: s, singlet; d, doublet; t, triplet; q, quartet; br, broad. [g] Not resolved. [h] The letters A, B, and C refer to the triphos phosphorus atoms, whereas D and E denote the P atoms of the triphenylphosphine ligands. [i] The fast exchange spectrum was recorded in CD_3NO_2. [j] This value was introduced to successfully reproduce the line width of the resonance in the spin simulation procedure.

Table II. Experimental Data for the X-Ray Diffraction Study of [(triphos)(Cl)Ir(μ-H){$Au_2(PPh_3)_2$}]PF_6·C_4H_8O (4·THF)

chem formula	$C_{81}H_{78}Au_2ClF_6IrOP_6$
mol wt	1989.83
space group	$P\bar{1}$ (No. 2)
a, Å	14.317 (6)
b, Å	17.626 (4)
c, Å	17.791 (2)
α, deg	90.82 (1)
β, deg	110.43 (2)
γ, deg	112.31 (2)
Z	2
V, Å^3	3836 (4)
$\rho_{(calcd)}$, g cm^{-3}	1.721
μ, cm^{-1}	57.454
T, °C	23
λ, Å	0.710 69 (graphite monochromated, Mo Kα)
decay correction factrs	0.990–1.191
transmission coeff	0.7704–0.9978
R[a]	0.041
R_w[b]	0.052

[a] $R = \sum||F_o|-(1/k)|F_c||/\sum|F_o|$. [b] $R_w = [\sum w(|F_o|-(1/k)|F_c|)^2]/\sum w|F_o|^2]^{1/2}$. $\sigma(F_o) = [\sigma^2(F_o)^2 + f^2(F_o)^2]^{1/2}/2F_o$.

minimized was $[\sum w(|F_o| - (1/k)|F_c|)]^2$ with $w = [\sigma^2(F_o)]^{-1}$, using anisotropic temperature factors for the Au, Ir, Cl, P, and F atoms and for the carbons of the triphos skeleton; isotropic B's were used for the others. No extinction correction was deemed necessary (the isotropic extinction parameter g was less than 2.2×10^{-9}).

The scattering factors used, corrected for the real and imaginary parts of the anomalous dispersion, were taken from the literature.[22]

Toward the end of the refinement a molecule of solvent (THF) was found and refined using isotropic temperature factors. The final Fourier difference map clearly showed a peak, in the expected position for a bridging hydride, that was also confirmed by calculating a Fourier with a limited data set ($\sin\theta/\lambda \leq 0.31$ Å^{-1}). This atom was therefore retained and successfully refined, although the esd's were high, as expected, using an isotropic temperature factor.

The contribution from the remaining hydrogens in their idealized positions (C–H = 0.95 Å, B_{iso} = 5.0 Å^2) was taken into account but not refined.

Upon convergence [no parameter shift ratio >0.08σ(p)] a Fourier difference map showed no significant feature. All calculations were carried out by using the MOLEN crystallographic package.[23] Final atomic coordinates and equivalent thermal factors are given in Table III.

Results

Synthesis and Characterization of the Monogold Adduct [(triphos)Ir(H)(C_2H_4){Au(PPh_3)}]PF_6 (3). The addition of 1 equiv of [Au(THF)(PPh_3)]PF_6 (prepared in situ from [AuCl(PPh_3)] and $TlPF_6$) to a THF solution of the hydrido ethylene complex [(triphos)Ir(H)(C_2H_4)] (**1**)[14] under a steady stream of ethylene produces a yellow solution from which pale yellow crystals of [(triphos)Ir(H)(C_2H_4){Au(PPh_3)}]PF_6 (**3**) are obtained in good yield by addition of an ethanol/*n*-heptane mixture.

Complex **3** can be synthesized also by substituting the octahedral (OCT) iridium(III) ethyl dihydride complex [(triphos)-Ir(H)$_2$(C_2H_5)] (**2**)[14] for **1**. Indeed, the dihydride **2** is stable in THF solution but readily eliminates ethane (GC or ^1H NMR detectable) upon interaction with [Au(THF)(PPh_3)]$^+$. The alternative path involving preliminary reaction with C_2H_4, followed by electrophilic attack by the gold fragment at the metal, is ruled out in light of the stability of **2** under ethylene.[24] The modification of the reactivity of polyhydridometal complexes with Lewis acids has been recently studied by Caulton, Chaudret, and

(22) *International Tables for X-Ray Crystallography*; Kynoch Press: Birmingham, U.K., 1974; Vol. IV.

(23) *MOLEN Structure Determination Package*; Enraf-Nonius: Delft, The Netherlands, 1990.

(24) Unpublished results from this laboratory.

Table III. Final Positional Parameters and Equivalent Thermal Factors for $[(triphos)(Cl)Ir(\mu\text{-}H)\{Au_2(PPh_3)_2\}]PF_6 \cdot C_4H_8O$ (4·THF)[a]

atom	x	y	z	B(A2)	atom	x	y	z	B(A2)
Au1	0.220 70 (4)	0.349 61 (3)	0.700 14 (3)	3.05 (1)	C311	0.2143 (9)	0.0808 (7)	0.8650 (7)	3.5 (3)*
Au2	0.266 15 (3)	0.211 04 (3)	0.728 85 (3)	3.03 (1)	C312	0.3163 (9)	0.1463 (7)	0.8959 (7)	3.4 (3)*
Ir	0.098 44 (3)	0.220 54 (3)	0.755 88 (3)	2.31 (1)	C313	0.408 (1)	0.1339 (8)	0.9489 (8)	4.1 (3)*
Cl	0.0082 (2)	0.1751 (2)	0.6075 (2)	3.73 (8)	C314	0.396 (1)	0.0545 (9)	0.9693 (9)	5.1 (3)*
Pf	0.0355 (3)	0.7159 (2)	0.8516 (3)	5.1 (1)	C315	0.291 (1)	−0.0119 (9)	0.9373 (9)	5.2 (3)*
P1	0.1791 (2)	0.2825 (2)	0.8881 (2)	2.68 (8)	C316	0.2025 (9)	0.0012 (8)	0.8872 (8)	3.9 (3)*
P2	−0.0693 (2)	0.1973 (2)	0.7629 (2)	2.90 (8)	C321	0.0309 (8)	0.0001 (7)	0.7172 (7)	3.1 (3)*
P3	0.0915 (2)	0.0925 (2)	0.7961 (2)	2.63 (8)	C322	0.0553 (9)	0.0081 (7)	0.6474 (7)	3.6 (3)*
P4	0.3058 (3)	0.4608 (2)	0.6515 (2)	3.36 (9)	C323	0.012 (1)	−0.0603 (8)	0.5859 (8)	4.7 (3)*
P5	0.3871 (2)	0.1697 (2)	0.7028 (2)	3.38 (8)	C324	−0.061 (1)	−0.1397 (9)	0.5957 (9)	5.4 (4)*
F1	0.1379 (7)	0.6951 (6)	0.8746 (6)	8.9 (3)	C325	−0.085 (1)	−0.1471 (9)	0.6639 (9)	5.3 (3)*
F2	−0.036 (1)	0.271 (1)	1.2333 (7)	14.8 (6)	C326	−0.040 (1)	−0.0755 (8)	0.7273 (8)	4.1 (3)*
F3	0.0698 (8)	0.2696 (8)	1.171 (1)	13.8 (5)	C411	0.454 (1)	0.5026 (8)	0.7031 (8)	4.3 (3)*
F4	−0.0364 (9)	0.2970 (8)	1.0603 (7)	11.4 (4)	C412	0.518 (1)	0.590 (1)	0.724 (1)	6.5 (4)*
F5	0.1068 (9)	0.8070 (6)	0.8884 (8)	11.2 (5)	C413	0.634 (1)	0.615 (1)	0.767 (1)	7.8 (5)*
F6	−0.040 (1)	0.6220 (7)	0.823 (1)	14.9 (6)	C414	0.675 (1)	0.556 (1)	0.786 (1)	7.5 (5)*
O(THF)	0.390 (3)	0.197 (2)	0.189 (2)	21 (2)*	C415	0.614 (1)	0.473 (1)	0.762 (1)	7.7 (5)*
C1(THF)	0.461 (3)	0.185 (2)	0.253 (3)	24 (2)*	C416	0.499 (1)	0.4436 (9)	0.720 (1)	6.0 (4)*
C2(THF)	0.462 (3)	0.113 (2)	0.204 (2)	19 (1)*	C421	0.266 (1)	0.5465 (8)	0.6586 (8)	4.2 (3)*
C3(THF)	0.334 (2)	0.070 (2)	0.166 (2)	15 (1)*	C422	0.263 (1)	0.5688 (9)	0.7329 (9)	5.5 (4)*
C4(THF)	0.285 (3)	0.135 (2)	0.175 (2)	19 (1)*	C423	0.232 (2)	0.634 (1)	0.744 (1)	8.8 (5)*
C1	0.1330 (9)	0.2059 (6)	0.9514 (6)	2.6 (3)	C424	0.189 (2)	0.666 (1)	0.677 (1)	11.8 (7)*
C2	−0.0689 (8)	0.1755 (7)	0.8651 (7)	3.1 (3)	C425	0.191 (2)	0.648 (2)	0.597 (2)	15 (1)*
C3	0.0045 (8)	0.0631 (7)	0.8567 (7)	3.3 (3)	C426	0.241 (2)	0.587 (1)	0.595 (1)	10.0 (6)*
C4	0.0135 (9)	0.1391 (7)	0.9116 (7)	3.4 (3)	C431	0.2790 (9)	0.4380 (7)	0.5442 (7)	3.5 (3)*
C5	−0.021 (1)	0.1027 (8)	0.9826 (7)	4.6 (4)	C432	0.176 (1)	0.3785 (8)	0.4955 (8)	4.3 (3)*
C111	0.3276 (8)	0.3310 (7)	0.9438 (7)	3.1 (3)*	C433	0.149 (1)	0.3615 (9)	0.4127 (9)	5.6 (4)*
C112	0.3930 (9)	0.3803 (7)	0.9048 (7)	3.8 (3)*	C434	0.223 (1)	0.4018 (9)	0.3785 (9)	5.8 (4)*
C113	0.508 (1)	0.4198 (8)	0.9469 (8)	4.9 (3)*	C435	0.330 (1)	0.4617 (9)	0.4280 (9)	5.7 (4)*
C114	0.557 (1)	0.4086 (9)	1.0253 (9)	5.4 (4)*	C436	0.356 (1)	0.4788 (8)	0.5115 (8)	4.7 (3)*
C115	0.490 (1)	0.362 (1)	1.0642 (9)	6.0 (4)*	C511	0.5131 (9)	0.1945 (7)	0.7904 (7)	3.7 (3)*
C116	0.374 (1)	0.3217 (8)	1.0239 (8)	4.6 (3)*	C512	0.556 (1)	0.2708 (8)	0.8409 (8)	5.0 (3)*
C121	0.1487 (9)	0.3707 (7)	0.9121 (7)	3.1 (3)*	C513	0.654 (1)	0.294 (1)	0.911 (1)	6.8 (4)*
C122	0.1365 (9)	0.4247 (7)	0.8556 (7)	3.4 (3)*	C514	0.700 (1)	0.237 (1)	0.931 (1)	6.6 (4)*
C123	0.118 (1)	0.4947 (8)	0.8768 (8)	4.5 (3)*	C515	0.659 (1)	0.161 (1)	0.882 (1)	6.1 (4)*
C124	0.114 (1)	0.5089 (8)	0.9499 (8)	4.2 (3)*	C516	0.561 (1)	0.1367 (8)	0.8087 (8)	4.5 (3)*
C125	0.125 (1)	0.4565 (9)	1.0058 (9)	5.6 (4)*	C521	0.3341 (9)	0.0591 (7)	0.6714 (7)	3.4 (3)*
C126	0.143 (1)	0.3862 (8)	0.9855 (8)	4.7 (3)*	C522	0.312 (1)	0.0240 (9)	0.5918 (9)	5.1 (3)*
C211	−0.1953 (9)	0.1106 (7)	0.6936 (7)	3.2 (3)*	C523	0.262 (1)	−0.063 (1)	0.567 (1)	6.8 (4)*
C212	−0.1921 (9)	0.0431 (7)	0.6567 (7)	3.6 (3)*	C524	0.235 (1)	−0.115 (1)	0.623 (1)	6.3 (4)*
C213	−0.289 (1)	−0.0274 (8)	0.6098 (8)	4.9 (3)*	C525	0.259 (1)	−0.0819 (9)	0.7007 (9)	5.9 (4)*
C214	−0.388 (1)	−0.0245 (9)	0.5994 (9)	5.8 (4)*	C526	0.306 (1)	0.0073 (8)	0.7249 (8)	4.9 (3)*
C215	−0.396 (1)	0.044 (1)	0.630 (1)	7.0 (4)*	C531	0.4278 (9)	0.2170 (7)	0.6231 (7)	3.4 (3)*
C216	−0.297 (1)	0.1140 (9)	0.6832 (9)	5.4 (4)*	C532	0.535 (1)	0.237 (1)	0.625 (1)	6.3 (4)*
C221	−0.1095 (9)	0.2849 (7)	0.7461 (7)	3.6 (3)*	C533	0.557 (1)	0.267 (1)	0.556 (1)	7.6 (5)*
C222	−0.102 (1)	0.3188 (8)	0.6770 (8)	4.7 (3)*	C534	0.479 (1)	0.283 (1)	0.494 (1)	7.1 (4)*
C223	−0.128 (1)	0.390 (1)	0.660 (1)	6.6 (4)*	C535	0.375 (1)	0.2678 (9)	0.4946 (9)	6.0 (4)*
C224	−0.158 (1)	0.422 (1)	0.715 (1)	7.1 (4)*	C536	0.350 (1)	0.2339 (9)	0.5604 (9)	5.8 (4)*
C225	−0.168 (1)	0.389 (1)	0.785 (1)	6.2 (4)*	HM	0.098 (9)	0.316 (7)	0.729 (7)	3 (3)*
C226	−0.141 (1)	0.3165 (8)	0.8008 (8)	4.3 (3)*					

[a] Esd's on the last significant digit are given in parentheses. Pf is the P atom of the anion; atoms labeled THF are those of the clathrated solvent molecule. Asterisks denote atoms that were refined isotropically. Anisotropically refined atoms are given in the form of the isotropic equivalent displacement parameter defined as $(4/3)[a_2B(1,1) + b_2B(2,2) + c_2B(3,3) + ab(\cos\gamma)B(1,2) + ac(\cos\beta)B(1,3) + bc(\cos\alpha)B(2,3)]$.

their co-workers.[25] It is expected that the interaction of **2** with a Lewis acid such as $[Au(PPh_3)]^+$ reduces the electron density at iridium, thus favoring the reductive elimination of ethane.

Complex **3** is diamagnetic and air stable in the solid state. It is soluble in polar organic solvents such as halocarbons, acetone, and THF where it slowly decomposes if exposed to air. In contrast, it is stable in deoxygenated solutions and behaves as a 1:1 electrolyte.

The IR spectrum of solid **3** (KBr plates) contains a sharp, medium-intensity band at 2047 cm^{-1}. Such an absorbance is typical of iridium complexes containing terminal hydride ligands.[14,26] Actually, although the majority of known gold–iridium hydrides exhibit bridging hydride ligands,[27-33] complexes containing the metal–gold–PPh_3 moiety have some precedents.[27,34-41] The high-energy absorption at 2047 cm^{-1} disappears in the IR spectrum of the deuterated isotopomer of **3**, $[(triphos)Ir(D)(C_2H_4)\{Au(PPh_3)\}]PF_6$ (**3**-d_1). No band in the

(25) He, X. H.; Fernandez-Baeza, J.; Chaudret, B.; Folting, K.; Caulton, K. G. *Inorg. Chem.* **1990**, *29*, 5000.

(26) (a) Crabtree, R. H. In *Comprehensive Coordination Chemistry*; Wilkinson, G., Gillard, R. D., McCleverty, J. A., Eds.; Pergamon Press: Oxford, England, 1987; Vol. 2, Chapter 19, pp 689–714. (b) Hlatky, G. G.; Crabtree, R. H. *Coord. Chem. Rev.* **1985**, *65*, 1. (c) Antiñolo, A.; Jalón, F. A.; Otero, A.; Fajardo, M.; Chaudret, B.; Lahoz, F.; López, J. A. *J. Chem. Soc., Dalton Trans.* **1991**, 1861.

(27) For an exhaustive review on polynuclear iridium hydrido complexes, see: Gomes Carneiro, T. M.; Matt, D.; Braunstein, P. *Coord. Chem. Rev.* **1989**, *96*, 49.

(28) Alexander, B. D.; Johnson, B. J.; Johnson, S. M.; Boyle, P. D.; Kann, N. C.; Mueting, A. M.; Pignolet, L. H. *Inorg. Chem.* **1987**, *26*, 3506.

(29) Socol, S. M.; Meek, D. W.; Glaser, R. *Polyhedron* **1989**, *8*, 1903.

(30) Lehner, H.; Matt, D.; Pregosin, P. S.; Venanzi, L. M.; Albinati, A. *J. Am. Chem. Soc.* **1982**, *104*, 6825.

(31) Albinati, A.; Anklin, C.; Janser, P.; Lehner, H.; Matt, D.; Pregosin, P. S.; Venanzi, L. M. *Inorg. Chem.* **1989**, *28*, 1105.

(32) Albinati, A.; Demartin, F.; Janser, P.; Rhodes, L. F.; Venanzi, L. M. *J. Am. Chem. Soc.* **1989**, *111*, 2115.

(33) Casalnuovo, A. L.; Laska, T.; Nilsson, P. V.; Olofson, J.; Pignolet, L. H.; Bos, W.; Bour, J. J.; Steggerda, J. J. *Inorg. Chem.* **1985**, *24*, 182.

(34) Casalnuovo, A. L.; Laska, T.; Nilsson, P. V.; Olofson, J.; Pignolet, L. H. *Inorg. Chem.* **1985**, *24*, 233.

(35) Luke, M. A.; Mingos, D. M. P.; Sherman, D. J.; Wardle, R. W. M. *Transition Met. Chem. (London)* **1987**, *12*, 37.

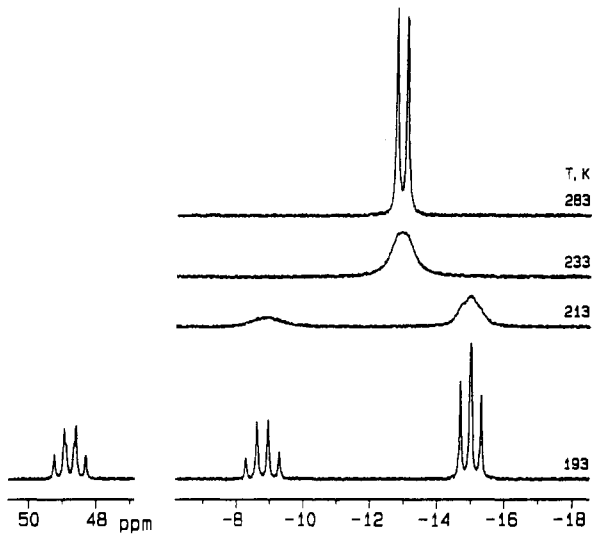

Figure 1. Variable-temperature $^{31}P\{^1H\}$ NMR spectra of **3** in CD_2Cl_2 (81.01 MHz, 85% H_3PO_4 reference).

IR spectrum of **3**-d_1 may be safely assigned to ν(Ir–D). Actually, for an expected $k_{H/D}$ value of 1.35–1.40, the ν(Ir–D) vibration would fall between 1510 and 1460 cm^{-1}, a region crowded by the vibrational absorptions of the triphos coligand.

Although the infrared spectrum of **3** does provide support for a terminal bonding mode of the hydride ligand, a detailed analysis of the VT NMR spectra of **3** (particularly the proton spectra) as well as IR measurements in solution are consistent with a bridging hydride formulation and, therefore, with a terminal to bridging-hydride tautomerization process on going from the solid state to solution (Scheme I). In particular, the IR spectrum of **3** in CH_2Cl_2 solution shows the disappearance of the band at 2047 cm^{-1}, whereas a new broader absorbance at 1609 cm^{-1} is clearly observable, which can be assigned to a bridging hydride ligand.[26] The presence of broad bands of lowered frequency in the IR spectrum of a hydride complex is considered as a reliable spectroscopic criterion for the identification of a μ-H interaction.[26] In the case at hand, this band provides evidence for the proposed solid-state/solution tautomerization process. The observed ν(Ir–$H_{terminal}$) → ν(Ir–$H_{bridging}$) IR shift is very large indeed (442 cm^{-1}), but not uncommon for mixed metal–gold hydrides.[26c]

The $^{31}P\{^1H\}$ NMR spectra recorded in CD_2Cl_2 in the temperature range +30 to −100 °C are reported in Figure 1. The low-temperature spectrum (−80 °C, lower trace) consists of three resonances, forming a first-order AB_2C splitting pattern (δ_A −8.80, δ_B −14.99, δ_C 48.76) with a 1:2:1 intensity ratio. The low-field signal, which appears as a doublet of triplets, is assigned to the gold phosphine atom (P_C) which couples to the three triphos phosphorus atoms, two of which (P_B) are magnetically equivalent. The larger value of the coupling constant to P_A [$^3J(P_AP_C)$ = 49.6 Hz; $^3J(P_BP_C)$ = 20.0 Hz] suggests a *transoid* disposition of the P_A–Ir–Au–P_C moiety.[13] The other signals, which resonate at negative fields, are due to the phosphorus nuclei of triphos and exhibit NMR parameters (chemical shifts and coupling constants) in line with those reported for other "[(triphos)Ir]" complexes.[14,32,42]

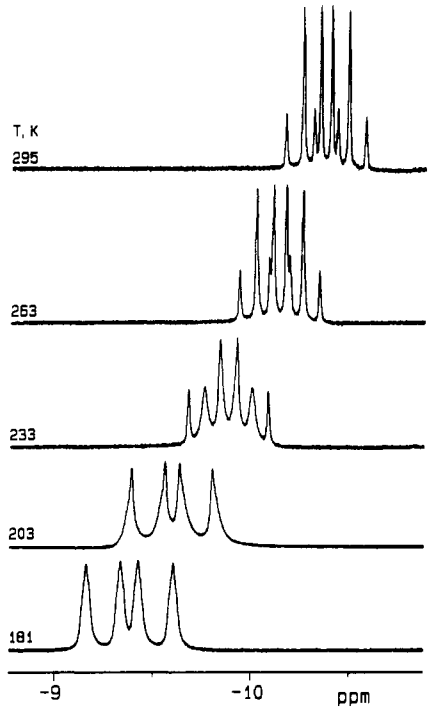

Figure 2. ^1H NMR spectrum of **3** in the hydride region at different temperatures (200.13 MHz, CD_2Cl_2, TMS reference).

At higher temperature, complex **3** shows a dynamic behavior which equilibrates the three triphos phosphorus atoms, averaging the P_A and P_B environments. Indeed, as the temperature is increased, the two triphos resonances broaden and then coalesce at about −50 °C. The fast exchange spectrum (see the upper trace in Figure 1) is attained at room temperature and consists of two distinct signals, forming an A_3B spin system [δ_A −13.02, δ_B 48.59, $^3J(P_AP_B)$ = 25.0 Hz]. The observed multiplicity is consistent with a complete scrambling of the P atoms of the polyphosphine.

In keeping with the $^{31}P\{^1H\}$ NMR spectral data, the ^1H NMR spectrum of **3** (CD_2Cl_2, 20 °C) in the hydride region exhibits a doublet of quartets (δ −10.37) which clearly confirms the presence of an iridium-bonded hydride ligand (Figure 2).

Valuable information for elucidating the solution structure of **3** is provided by the values of the geminal coupling constants $^2J(HP_B)$ and $^2J(HP_A)$ which are 43.2 and 26.5 Hz, respectively (confirmed by selective decoupling of the ^{31}P environments). In a recent review, Pignolet and co-workers have addressed the question of relating the presence of bridging (M–H–AuPPh$_3$) or terminal (H–M–AuPPh$_3$) hydrides with the magnitude of the ^2J(H–Au–P) coupling constant.[13] According to their analysis, it is agreed that this coupling is larger than 20 Hz for bridging hydrides and very dependent on the H–Au–P angle in solution.[13,28,33,43]

(36) Alexander, B. D.; Johnson, B. J.; Johnson, S. M.; Casalnuovo, A. L.; Pignolet, L. H. *J. Am. Chem. Soc.* **1986**, *108*, 4409.
(37) See footnote 56 in ref 13: Casalnuovo, A. L. Ph.D. Dissertation, University of Minnesota, 1984.
(38) Alexander, B. D.; Boyle, P. D.; Johnson, B. J.; Johnson, S. M.; Casalnuovo, A. L.; Mueting, A. M.; Pignolet, L. H. *Inorg. Chem.* **1987**, *26*, 2547.
(39) Casalnuovo, A. L.; Pignolet, L. H.; van der Velden, J. W. A.; Bour, J. J.; Steggerda, J. J. *J. Am. Chem. Soc.* **1983**, *105*, 5957.
(40) Calsanuovo, A. L.; Casalnuovo, J. A.; Nilsson, P. V.; Pignolet, L. H. *Inorg. Chem.* **1985**, *24*, 2554.
(41) For other polynuclear complexes containing iridium–gold bonds, see: (a) Balch, A. L.; Catalano, V. J.; Olmstead, M. M. *J. Am. Chem. Soc.* **1990**, *112*, 2010. (b) Hutton, A. T.; Pringle, P. G.; Shaw, B. L. *Organometallics* **1983**, *2*, 1889. (c) Balch, A. L.; Catalano, V. J.; Olmstead, L. M. *Inorg. Chem.* **1989**, *29*, 585. (d) Braga, D.; Grepioni, F.; Livotto, F. S.; Vargas, M. D. *J. Organomet. Chem.* **1990**, *391*, C28. (e) Sykes, A. G.; Mann, K. R. *J. Am. Chem. Soc.* **1990**, *112*, 7247.
(42) (a) Bianchini, C.; Meli, A.; Peruzzini, M.; Vizza, F. *J. Am. Chem. Soc.* **1990**, *112*, 6726. (b) Bianchini, C.; Caulton, K. G.; Chardon, C.; Eisenstein, O.; Folting, K.; Johnson, T. J.; Meli, A.; Peruzzini, M.; Rauscher, D. J.; Streib, W. E.; Vizza, F. *J. Am. Chem. Soc.* **1991**, *113*, 5127. (c) Janser, P.; Venanzi, L. M.; Bachechi, F. *J. Organomet. Chem.* **1985**, *296*, 229. (d) McGilligan, B. S.; Venanzi, L. M.; Wolfer, M. *Organometallics* **1987**, *6*, 946. (e) Geerts, R. L.; Huffman, J. C.; Westerberg, D. E.; Folting, K.; Caulton, K. G. *New J. Chem.* **1988**, *12*, 455. (f) Arpac, E.; Dahlenburg, L. *Chem. Ber.* **1985**, *118*, 3188. (g) Siegl, W. O.; Lapporte, S. J.; Collman, J. P. *Inorg. Chem.* **1971**, *10*, 2158.

Values higher than 100 Hz have been found for an approximately trans arrangement. As an example, in the X-ray authenticated complex $[AuCr(\mu\text{-}H)(CO)_5(PPh_3)]$, a $^2J(HP_{Au})$ of 105 Hz is associated with an H–Au–P bond angle of ca. 170°.[44] In our case, the magnitude of the $^2J(HP_B)$ coupling constant (43.2 Hz) is consistent with the presence of a hydrido-bridged system. On the other hand, its relatively low value suggests that the bulky $AuPPh_3$ fragment may not be rigid with respect to the gold hydride vector. In light of the observed fluxionality, it is reasonable to have found a smaller spin–spin coupling than would be expected for a trans μ-H–Au–PPh_3 stereochemistry.

The other geminal coupling constant [$^2J(HP_A)$ = 26.5 Hz] lies midway between the values observed for the parent derivative **1** [$^2J(HP_{trans})$ = 143.6, $^2J(HP_{cis})$ = 12.6 Hz] which is static on the NMR time scale,[14] and agrees well with data reported for other stereochemically nonrigid five-coordinate (triphos)Ir complexes (see for example the highly fluxional complex [(triphos)Ir(H)(CO)] for which a $^2J(HP)$ of 20.7 Hz has been reported).[42c]

The dynamic structure proposed for **3** is also supported by the analysis of the aliphatic region of the spectrum which consists of three well-separated resonances of a 6:4:3 intensity ratio. A filled-in doublet at 2.55 ppm and a quartet of half-intensity at δ 1.57 are typical of triphos complexes in the fast motion regime and are assigned to the six methylenic protons and to the methyl group [$^2J(HP)$ = 3.1 Hz] of the ligand backbone, respectively.[14,45] In between the two triphos resonances a broad singlet of 4 H intensity at δ 2.28 indicates the presence of a dynamic ethylene ligand.[14,45]

Upon a decrease in the temperature, the dq pattern of the hydride ligand at −10.37 ppm moves downfield (at −80 °C, δ −9.38), broadens, and then transforms into a broad doublet of doublets whose components resolve in four very broad triplets by applying the Gaussian multiplication procedure. The temperature dependence of the chemical shift follows the first-order equation δ (ppm) = $-10.196 - 8.789 \times 10^{-3}t$ (°C).

In a similar way, the ethylene resonance coalesces at ca. −40 °C and then emerges from the baseline as two broad humps of the same intensity (2 H) which are consistent with an almost static ethylene ligand (at −80 °C, δ 3.99 and 0.99).

Particularly informative for elucidating the low-temperature structure of **3** is the analysis of the geminal heteronuclear coupling constants (confirmed by selective decoupling of the ^{31}P resonances) involving the hydride proton [$^2J(HP_C)$ = 52.6, $^2J(HP_A)$ = 79.9, $^2J(HP_B) \leq 2$ Hz]. Such coupling constants are consistent with a significant freezing out of the scrambling process. In particular, notwithstanding the value of $^2J(HP_A)$ increases, it never approaches the values reported for authenticated hydrides of iridium having an almost regular trans disposition of the H–Ir–P moiety [see for example $^2J(HP_{trans})$ = 143.6 Hz in the parent complex **1**].[14] At the same time, the spin–spin coupling constant to the gold phosphine atom, $^2J(HP_C)$, slightly increases with respect to the room temperature value, but remains far away from the values expected for dinuclear gold–iridium hydrides with a trans arrangement of the H–Au–P_C moiety.[13]

The $^{13}C\{^1H\}$ NMR spectrum of **3** (CD_2Cl_2, 20 °C) is consistent with the presence of a dynamic ethylene ligand and exhibits a single signal at δ 19.85 for the two equivalent ethylene carbons.

Table IV. Selected Bond Lengths (Å) and Bond Angles (deg) for the cation $[(triphos)(Cl)Ir(\mu\text{-}H)\{Au_2(PPh_3)_2\}]^+$ [a]

Ir–Au1	2.7343 (7)	Au1–Ir–P2	127.03 (9)
Ir–Au2	2.6709 (7)	Au2–Ir–P3	78.85 (8)
Au1–Au2	2.7676 (7)	Au1–Ir–P1	96.02 (8)
Ir–Cl	2.461 (3)	Au2–Ir–P1	101.71 (8)
Ir–P1	2.265 (3)	Au1–Ir–Cl	77.78 (8)
Ir–P2	2.327 (3)	Au2–Ir–Cl	81.85 (8)
Ir–P3	2.354 (3)	P1–Ir–Cl	170.5 (1)
Au1–P4	2.254 (3)	Au2–Ir–P2	166.66 (8)
Au1–P5	2.292 (3)	Ir–H–Au1	97 (6)
Ir–H	1.8 (1)	P3–Ir–H	176 (4)
Au1–H	1.9 (1)	Ir–Au1–Au2	58.08 (2)
		Ir–Au2–Au1	60.33 (2)
		Au1–Ir–Au2	61.59 (2)
		Ir–Au1–P4	173.4 (1)
		Ir–Au2–P5	166.4 (1)
		Au1–Au2–P5	132.0 (1)
		Au2–Au1–P4	128.3 (1)

[a] Esd's are given in parentheses.

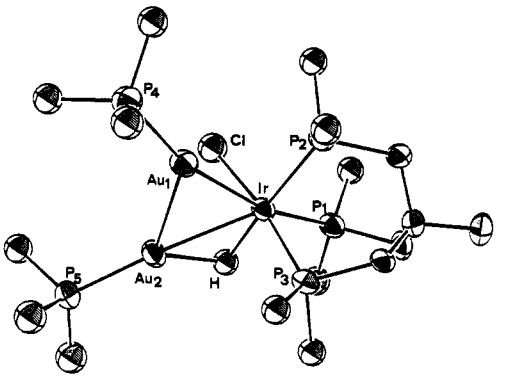

Figure 3. ORTEP drawing of the complex cation $[(triphos)(Cl)Ir(\mu\text{-}H)\{Au_2(PPh_3)_2\}]^+$. Only the ipso carbon atom of each phenyl ring has been reported in the drawing.

Synthesis and Characterization of the Digold Adducts $[(triphos)(Cl)Ir(\mu\text{-}H)\{Au_2(EPh_3)_2\}]PF_6$, [E = P (4), As (5)]. The reaction of **3** with 1 equiv of $[AuCl(PPh_3)]$ yields the $IrAu_2$ cluster $[(triphos)(Cl)Ir(\mu\text{-}H)\{Au_2(PPh_3)_2\}]PF_6$ (**4**) and 1 equiv of C_2H_4 (GC or ^1H NMR detectable). Compound **4** can be prepared also by a one-pot reaction between the iridium hydrides **1** or **2**, a double proportion of the gold reagent $[AuCl(PPh_3)]$, and a slight excess of NH_4PF_6 to metathesize the chloride counteranion. A 1-equiv portion of ethylene or of ethane is evolved depending on the precursor used (Scheme I).

The arsino analogue of **4**, i.e., $[(triphos)(Cl)Ir(\mu\text{-}H)\{Au_2(AsPh_3)_2\}]PF_6$ (**5**), is similarly prepared by substituting $[AuCl(AsPPh_3)]$ for $[AuCl(PPh_3)]$.

Compounds **4** and **5** appear as lemon yellow crystals which are air stable in both the solid state and in solution where they behave as 1:1 electrolytes.

A single-crystal X-ray diffraction analysis has been carried out on compound **4**.

The crystal structure of **4** consists of a discrete $(triphos)(Cl)Ir(\mu\text{-}H)\{Au_2(PPh_3)_2\}]^+$ cation, a PF_6 anion, and a clathrated THF molecule; the packing is dictated by van der Waals interactions, with no unusual intramolecular contacts.

A selected list of bond lengths and angles is given in Table IV, while an ORTEP view is presented in Figure 3.

The iridium and gold atoms are bonded to each other, forming the core of a triangular cluster with a hydrogen atom bridging an Ir–Au edge. If one considers the Ir–H–Au triangle as ideally arising from the protonation of an Ir–Au bond, then the coordination around iridium may be described as a distorted octahedron consisting of the triphos ligand, occupying one of the trigonal faces, a chlorine ligand, and two gold atoms.

The Ir–Au bond lengths, 2.6709 (7) and 2.7343 (7) Å, respectively, fall in the expected range.[31,33,35-37,40,41e] The longer

(43) Alexander, B. D.; Gomez-Sal, M. P.; Gannon, P. R.; Blaine, C. A.; Boyle, P. D.; Mueting, A. M.; Pignolet, L. H. *Inorg. Chem.* **1988**, *27*, 3301.
(44) Green, M.; Orpen, A. G.; Salter, I. A.; Stone, F. G. A. *J. Chem. Soc., Dalton Trans.* **1984**, 2497.
(45) (a) Bianchini, C.; Meli, A.; Peruzzini, M.; Vizza, F.; Frediani, P.; Ramirez, J. A. *Organometallics* **1990**, *9*, 226. (b) Bianchini, C.; Meli, A.; Peruzzini, M.; Vizza, F.; Albinati, A. *Organometallics* **1990**, *9*, 2283. (c) Thaler, E. G.; Caulton, K. G. *Organometallics* **1990**, *9*, 1871. (d) Thaler, E. G.; Folting, K.; Caulton, K. G. *J. Am. Chem. Soc.* **1990**, *112*, 2664. (e) Johnston, G. G.; Baird, M. C. *Organometallics* **1989**, *8*, 1894. (f) Rhodes, L. F.; Sorato, C.; Venanzi, L. M.; Bachechi, F. *Inorg. Chem.* **1988**, *27*, 604. (g) Ott, J.; Venanzi, L. M.; Ghilardi, C. A.; Midollini, S.; Orlandini, A. *J. Organomet. Chem.* **1985**, *291*, 89.

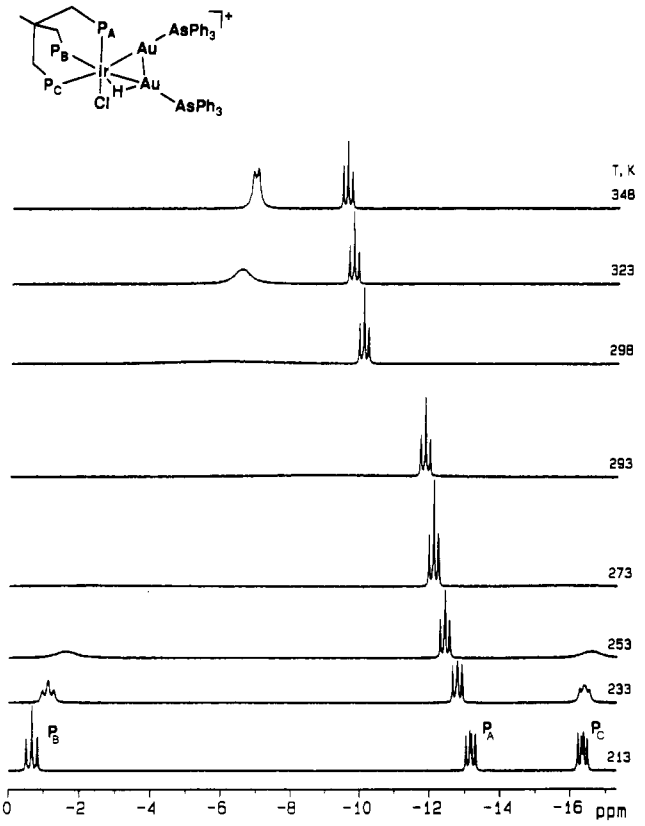

Figure 4. Variable-temperature $^{31}P\{^1H\}$ NMR spectra of **5** in CD_2Cl_2 (213–293 K) and CD_3NO_2 (298–348 K) (121.42 MHz, 85% H_3PO_4 reference).

bond distance corresponds to that of the Ir–H–Au edge. Similar metal–gold separations have been found in other heterometallic complexes having bridging hydrides, e.g., 2.697 (1) and 2.673 (1) in $[IrAu_2(H)(PPh_3)_4(NO_3)]BF_4$.[33]

The Ir–P bond distances are unequal due to the different trans influence of the various coligands; thus, the longest value [2.354 (3) Å] is found trans to the bridging H ligand and the shortest [2.265 (3) Å] trans to the chlorine ligand. The Au–Au separation, 2.7676 (7) Å, matches the expected value[12g,33,39,46] and is shorter than the value found in metallic gold.[47]

The Ir–H and Au–H bond distances are almost equal given the high esd's, while the Au–H–Ir angle [97 (1)°] is acute as expected for a "closed" three-center–two-electron interaction[48] and consistent with the short Au–Ir separation.

An alternative and intriguing description of the coordination around the iridium atom may be given considering the isolobal relationship between "Au_2" and H_2.[12] Accordingly, the iridium atom may be viewed as coordinated to interacting H_2 and H groups, i.e., an open pseudo-H_3 ligand (see below).

In nice accord with the solid-state structure, the IR spectra of **4** (Nujol mull) and of the arsino analogue **5** contain a weak and broad absorption at 1813 cm^{-1} which can be associated with the presence of a bridging hydride ligand.[26,32]

Both **4** and **5** are highly fluxional on the NMR time scale in the temperature range from +93 to −92 °C, and the limiting spectra are attained at comparable temperatures for the two compounds. The variable-temperature $^{31}P\{^1H\}$ NMR spectra of **5** and **4** are presented in Figures 4 and 5, respectively, together with the labeling scheme used in the NMR analysis.

The presence of as many as five magnetically active nuclei in **4** makes its VT ^{31}P spectra very complicated and hard to compute

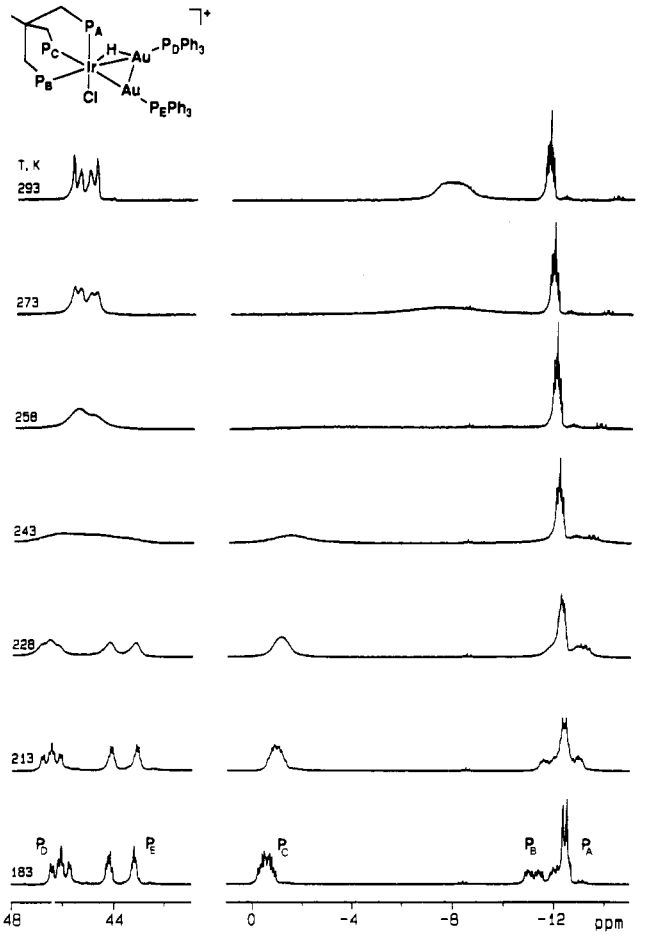

Figure 5. Variable-temperature $^{31}P\{^1H\}$ NMR spectra of **4** in CD_2Cl_2 (121.42 MHz, 85% H_3PO_4 reference).

by the currently available programs. In contrast, the variable-temperature spectra of the arsino analogue **5** are evidently much simpler and have successfully been simulated. The fast exchange spectrum for complex **5** is attained at 75 °C in CD_3NO_2. It consists of a first-order AB_2 splitting pattern with chemical shifts and coupling constants [δ_A −9.5, δ_B −6.92, $^2J(P_AP_B)$ = 16 Hz] in line with other OCT (triphos)Ir complexes in which the two equatorial ligands are chemically equivalent or are made equivalent by a dynamic process.[14,42] When the temperature is decreased, the resonance due to the phosphorus atom trans to the chloride ligand (P_A) does not broaden but shifts high field [δ_A (ppm) = $-12.142 + 2.300 \times 10^{-2}t$ (°C)]. In contrast, the other resonance, which is assigned to the two P_B atoms lying trans to the digold moiety, undergoes a dynamic process that causes coalescence of the signal just below room temperature. On decreasing the temperature further, two new resonances emerge from the coalescence of P_B that, at −60 °C, resolve into the BC part of an ABC spin system. Such a $^{31}P\{^1H\}$ NMR pattern is typical of OCT (triphos)Ir complexes having chemically non-equivalent ligands on the polyhedron face opposite to that capped by the triphosphine.[14,42] The exchange mechanism that equilibrates the two equatorial phosphorus atoms (P_B) has been studied by DNMR3 spectroscopy assuming exchange between the ABC and ACB configurations. A reliable simulation of the variable-temperature spectra of **5** has been obtained by using T_2 = 0.08 s and the following constants k (s^{-1}): 380 000 at 93 °C, 80 000 at 50 °C, 12 000 at 25 °C, 9000 at 20 °C, 1400 at 0 °C, 200 at −20 °C, 25 at −40 °C, and 1 at −60 °C. An Arrhenius plot of ln k vs $1/T$ results in a straight line from which the activation parameters from $\Delta H^\ddagger$ = 13.2 ± 0.2 kcal mol^{-1} and $\Delta S^\ddagger$ = 4.7 ± 0.6 cal K^{-1} mol^{-1} can be calculated. At the coalescence point (25 °C), a $\Delta G^\ddagger$ value of 11.8 ± 0.3 kcal mol^{-1} is found.

(46) Braunstein, P.; Lehner, H.; Matt, D.; Tiripicchio, A.; Tiripicchio Camellini, M. *Angew. Chem., Int. Ed. Engl.* **1984**, *23*, 304.
(47) Pearson, W. B. *Lattice Spacing and Structure of Metals and Alloys*; Pergamon Press: London, U.K., 1958; p 123.
(48) Teller, R. G.; Bau, R. *Struct. Bonding (Berlin)* **1981**, *44*, 1.

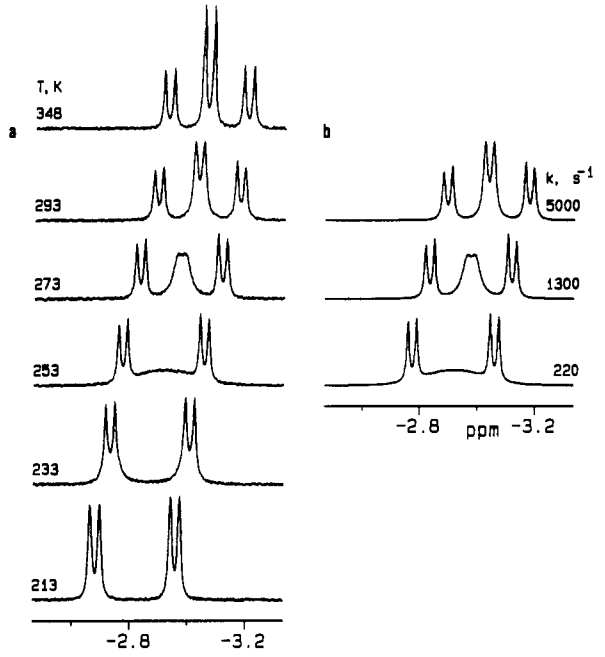

Figure 6. Variable-temperature ^1H NMR spectra of **5** (hydride region) in CD_2Cl_2 (299.94 MHz, TMS reference): (a) experimental spectra, (b) calculated spectra for the indicated exchange rates (k (s^{-1})), T_2 = 0.14 s.

A quite similar behavior is shown by **4** (Figure 5) whose NMR spectra are complicated by the presence of two additional NMR active nuclei. In particular, the $^{31}P\{^1H\}$ NMR spectrum of **4** transforms from an ABB'CC' splitting pattern into an ABCDE spin system on going from the fast motion regime (20 °C) to the slow motion regime (−92 °C). The low-temperature spectrum has successfully been computed using the following parameters: δ_A −12.48, δ_B −11.74, δ_C 0.59, δ_D 46.07, δ_E 43.67, $^2J(P_AP_B)$ = 14.1, $^2J(P_AP_B)$ = 19.4, $^3J(P_AP_D)$ = 2.4, $^3J(P_AP_E)$ = −10.3, $^2J(P_BP_C)$ = 20.6, $^3J(P_BP_D)$ = 50.4, $^3J(P_BP_E)$ = 122.9, $^3J(P_CP_D)$ = 36.3, $^3J(P_CP_E)$ = 11.2, $^3J(P_DP_E)$ = 11.9 Hz, T_2 = 0.2 s. On the basis of the chemical shift, one can readily assign the two low-field multiplets to the gold phosphine phosphorus atoms (P_D and P_E)[13] and the three signals at negative fields to the three nonequivalent triphos phosphorus atoms.[42] It is worth pointing out that the AuP_E fragment seems to be located almost trans to the P_B triphos phosphorus atom [$^3J(P_BP_E)$ = 122.9 Hz].[49]

The ^1H NMR spectra of **4** and **5** have been recorded at variable temperatures (−92 to +90 °C) in either CD_2Cl_2 or CD_3NO_2 within the appropriate temperature windows. Of particular interest is the presence in both spectra of a hydride resonance [at 20 °C in CD_2Cl_2, δ_H −2.78 (**4**), δ_H −3.04 (**5**)] that, in keeping with the solid-state IR spectra, is consistent with a bridging coordination mode.[50]

The experimental hydride resonance of **5** at different temperatures is reported in Figure 6 along with the simulated spectra. In the fast-exchange limit (>30 °C, CD_3NO_2) the spectrum consists of an AB_2X spin system (X = Ir-μ-*H*-Au) which transforms into an ABCX pattern on decreasing the temperature (<−40 °C, CD_2Cl_2). The dynamic process which exchanges the P_B and P_C environments has been simulated by a DNMR3 line shape analysis. The results of this study nicely fit with those figured out from the $^{31}P\{^1H\}$ NMR spectra and provide almost identical activation parameters. The slow-exchange spectrum (−60 °C), which shows a broad doublet of doublets for the hydride resonance, has been computed by using the following parameters: δ_H −2.75, $^2J(HP_A)$ = −9.0 Hz, $^2J(HP_B)$ = 83.9 Hz, $^2J(HP_C)$ ≤ 0.8 Hz (T_2 = 0.14 s). Selective heteronuclear decoupling experiments allow one to evaluate the geminal, $^2J(HP)$, coupling constants. Of particular relevance is the magnitude of the P_B–Ir–*H*–Au coupling constant (83.9 Hz) which matches the value found in the static structure of **3** [$^2J(HP_{trans})$ = 79.9 Hz] and, therefore, provides evidence supporting the solution structure proposed for the monogold adduct **3**.

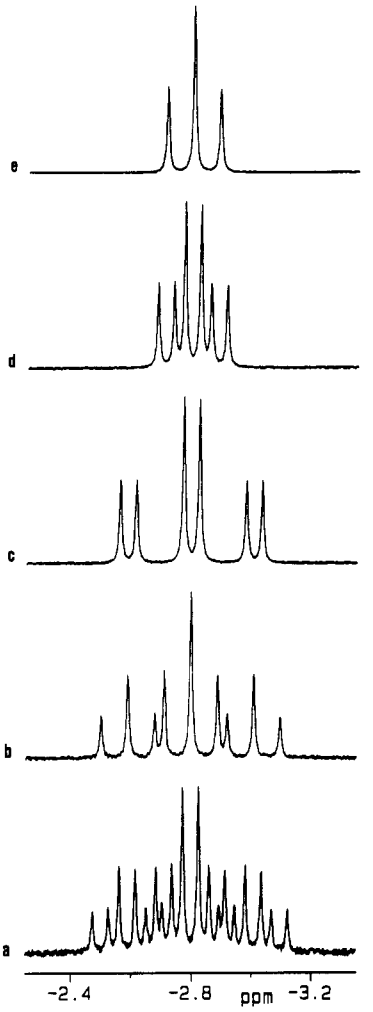

Figure 7. ^1H NMR spectra of **4** in the hydride region (200.13 MHz, CD_2Cl_2 TMS reference): (a) ^{31}P coupled spectrum; (b) ^{31}P decoupled at the gold–phosphine resonance (P_C); (c) ^{31}P decoupled at the triphos–P_B resonance; (d) ^{31}P decoupled at the triphos–P_A resonance; (e) ^{31}P decoupled at the triphos P_A and P_B resonances.

The ^1H NMR spectrum of **4** in the hydride region is presented in Figure 7 together with related spectra obtained by selective decoupling of the different phosphorus resonances.

Inspection of Figure 7 readily shows that the ^1H NMR spectrum of **4** is strictly related to that of **5**. At room temperature (fast-exchange limit), the high-field resonance (see lower trace in Figure 7) at δ_H −2.78 appears as an 18-line pattern with a relative intensity pattern of the type 1:1:2:2:1:2:1:2:4:4:2:1:2:1:2:2:1:1. The observed multiplicity arises from three coupling connections of the hydride with three different types of phosphorus atoms. Selective irradiation of the low-field absorbance (P_C) produces a triplet of doublets [$^2J(HP_B)$ = 40.8 Hz, $^2J(HP_A)$ = 10.5 Hz] (trace c in Figure 7), which closely resembles the hydride resonance in the fast-exchange spectrum of **5** (see Figure 6). A similar splitting pattern (trace d in Figure 7) is observed on decoupling the triphos P_B resonance [$^2J(HP_C)$ = 15.8 Hz]. Finally, the $^1H\{^{31}P_A\}$ spectrum (trace b in Figure 7) eliminating the small halving of each multiplet component is consistent with a residual BB'CC'X spin system.

(49) (a) Peter, M.; Peringer, P.; Müller, E. P. *J. Chem. Soc., Dalton Trans.* **1991**, 2459. (b) Pregosin, P. S.; Kunz, R. W. In *^{31}P and ^{13}C NMR of Transition Metal Phosphine Complexes*; Diehl, P., Fluck, E., Kosfeld, R., Eds.; Springer-Verlag: Berlin, Germany, 1979.

(50) Boron, P.; Musco, A.; Venanzi, L. M. *Inorg. Chem.* **1982**, *21*, 4192.

On lowering the temperature, a dynamic process similar to that observed for **5** takes place. As a result, the hydride resonance moves slightly downfield (at −92 °C, δ_H −2.60) and transforms into a very broad doublet of doublets. Each component of this low-temperature multiplet does not resolve into fine structure even when a Gaussian multiplication procedure is applied. This may be due to an incomplete freezing out of the scrambling process. Again, selective decoupling of the phosphorus resonances allows one to assign the larger coupling to P_B and the smaller one to the gold-bonded phosphorus atom (P_E) [$^2J(HP_B)$ = 87.5 Hz, $^2J(HP_E)$ = 40.0 Hz].

The T_1 value exhibited by **4** (245 ± 5 ms in CD_2Cl_2, 20 °C, 300 MHz, inversion recovery sequence) well matches the value measured for **3** in analogous experimental conditions (270 ± 5 ms). In contrast, the T_1 value for the hydride ligand in the starting complex **1** is significantly longer (360 ± 5 ms). The different T_1 values observed for the hydride ligands in **1**, **3**, and **4** can be ascribed to the different bonding mode of the H ligand in these compounds, i.e., terminal vs bridging. In particular, an additional and significant gold–hydrogen dipole–dipole contribution to the relaxation mechanism is expected to shorten the T_1 of the hydride ligand in the μ-H complexes **3** and **4** as compared to the terminal hydride complex **1**.[51]

Discussion

Comparison between Solid- and Solution-State Stereochemistry of 3. The most interesting feature coming out from the characterization of **3** is that the solution stereochemistry does not agree with the solid-state stereochemistry for which IR spectroscopy points to the presence of a terminal hydride ligand (Scheme I). In fact, on the basis of NMR and solution IR data, one can reasonably describe the solution structure of **3** as a trigonal bipyramid where the iridium center is coordinated to the three phosphorus atoms of triphos, to an ethylene molecule, and to an intact $HAuPPh_3$ unit via the Au–H bond. According to the analysis of the J_{PP} values, the ethylene ligand would occupy an equatorial position while the Ph_3P–Au–H unit must be located trans to one phosphorus atom of triphos. Such a structure well accounts for the dynamic behavior of the complex in solution which is typical of five-coordinate (triphos)metal complexes. In particular, a quite similar fluxionality is exhibited by the related bis(ethylene) complex $[(triphos)Ir(C_2H_4)_2]^+$.[14] Also, it is worth mentioning that the transfer of electron density from metal to ethylene π^* could be the driving force to form the Au–H bond. Indeed, such a transfer is expected to stabilize a trigonal-bipyramidal structure where the apical ligand [i.e., the (PPh_3-Au–H] receives fewer electrons.

Breakup of the Au–H bond occurs in the solid state. By analogy to the related dihydride $[(triphos)Ir(C_2H_4)(H)_2]^+$,[14] one may propose an octahedral geometry around iridium in **3** in which the H and $AuPPh_3$ groups lie cis to each other in the equatorial plane (Scheme I).

Well-documented terminal to bridging hydride tautomerizations of the type exhibited by **3** have not been reported yet. However, potential energy modeling techniques used for indirect location of hydride ligands in cluster compounds[52a] have provided evidence of a very low energy barrier separating bridging and terminal bonding modes of hydrides in mixed metal–gold cluster compounds.[13] It is therefore reasonable to conclude that the dissolution process of **3** may provide enough energy to promote the hydride rearrangement between the terminal-bridging coordination modes.

(51) (a) Gusev, D. G.; Vymenits, A. B.; Bakhmutov, V. I. *Inorg. Chem.* **1991**, *30*, 3116. (b) Desrosiers, P. J.; Cai, L.; Lin, Z.; Richards, R.; Halpern, J. *J. Am. Chem. Soc.* **1991**, *113*, 4173.

(52) (a) Orpen, A. G. *J. Chem. Soc., Dalton Trans.* **1980**, 2509. (b) Powell, J.; Gregg, M. R.; Sawyer, J. F. *J. Chem. Soc., Chem. Commun.* **1987**, 1029.

Scheme II

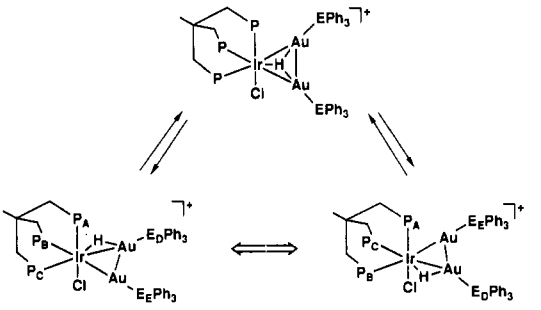

Also, a case of bridging-terminal hydrido equilibrium in a series of iron–platinum bimetallic complexes has been reported to occur in solution.[52b] It is therefore reasonable to conclude that the dissolution process of **3** may provide enough energy to promote the hydride rearrangement between the terminal-bridging coordination modes.

The question of addressing the bonding mode of the hydride ligand in **3** in both the solid state and in solution is of particular interest given the close analogy existing between molecular hydrogen complexes and transition-metal–gold hydrides. In fact, it is well known that the hydride ligand and the $Au(PR_3)$ fragment form a couple of isolobal analogues.[12] In light of the isolobal theory, it is intriguing to think of the solid-state ↔ solution rearrangement exhibited by **3** as due to an interconversion between "classical" and "nonclassical" forms of the H–$Au(PPh_3)$ ligand.

Solution Stereochemistry and Dynamic Behavior of 4 and 5. The dynamic behavior shown by the iridium–digold complexes **4** and **5** in solution may be interpreted as due to a scrambling process which averages the P_B and P_C environments and also exchanges the relative positions of the two gold phosphine (or arsine) moieties. It is worth stressing that the P_A atom (lying trans to the chloride ligand) does not take part in the exchanging process as we do not observe any broadening of the ^{31}P resonance of P_A within the temperature window under investigation (+93 to −92 °C).

In principle, the fluxional process shown by **4** and **5** may proceed via either intramolecular or dissociative mechanisms. However, the dissociative process where exchange between coordinated and free $Au(PPh)_3^+$ fragments would occur can be ruled out because (i) the presence of added $[Au(THF)(PPh_3)]^+$ does not affect the $^{31}P\{^1H\}$ NMR spectra at different temperatures and (ii) we observe retention of the μ-*H*–Au–P coupling in the fast motion regime. Furthermore, the occurrence of an intramolecular mechanism is strongly supported by the activation parameters, particular by the value of the entropy of activation (ΔS^* = 4.7 ± 0.6 cal K^{-1} mol^{-1}) which excludes a dissociative transition state. In conclusion, the most probable mechanism for the observed exchange process is the intramolecular one involving the shift of the hydride ligand from one Ir–Au edge of the IrAuAu triangle to the other one, so as to produce two indistinguishable structures. Once the occurrence of an intramolecular exchange of this type is taken for granted, it is reasonable to conclude that the hydrogen atom moves from one Ir–Au edge to the other with retention of contact with the metals. In fact, (i) no deuterium–hydrogen exchange occurs when the ^1H NMR spectra of **4** or **5** are recorded in the presence of D_2O or MeOD and (ii) the ΔS^* value would be much more positive in the case of a dissociative path.

It may also be possible that, at high temperatures, when the scrambling is fast on the NMR time scale, the dynamic process proceeds via a transition state where a hydride is triply bridging the $IrAu_2$ triangle (Scheme II). Indeed, several examples of transition-metal hydrides containing a μ_3-H ligand have been reported in the literature, including the trinuclear hydrido-bridged

Chart I

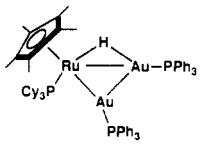

6

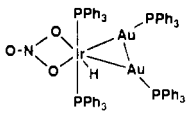

7

iridium complex $[Ir_3(\mu_3\text{-}H)(\mu\text{-}H)_3(H)_3(dppp)_3](BF_4)_2$[53] [dppp = 1,3-bis(diphenylphosphino)propane] and the iridium–disilver derivative $[(Ph_3P)_3Ir(\mu_3\text{-}H)(\mu\text{-}H)_2Ag_2(OSO_2CF_3)(OH_2)](OSO_2CF_3)$.[54]

Clusters of the type of **4** and **5** have very few precedents in transition-metal gold chemistry. Chaudret et al. have recently reported the preparation and characterization of the NMR static, neutral complex $[(\eta\text{-}C_5Me_5)\{(C_6H_{11})_3P\}Ru(\mu\text{-}H)\{Au(PPh_3)\}_2]$ (**6**), but no X-ray data are available (Chart I).[26c] Pignolet et al. reported the X-ray structure of $[IrAu_2(H)(PPh_3)_4(NO_3)]BF_4$ (**7**) without being able to precisely determine the bonding mode of the hydride ligand.[33] In fact, while NMR measurements were diagnostic for a terminal hydride stereochemistry, potential energy calculations based on the X-ray coordinates of the non-hydrogen atoms indicated that a bridging hydride may be nicely accommodated over one of the two iridium–gold bonds. Unfortunately, the hydride ligand could not be located by X-ray methods.[13,33]

As a final consideration, we draw the reader's attention to the electronic nature of the η^3-H–Au(EPh_3)–Au(EPh_3) ligand in **4** and **5**. In terms of the isolobal relationship, the H–Au(EPh_3)–Au(EPh_3) array is electronically analogous to the trihydrogen ligand for which convincing experimental evidence has not been reported yet.[55] Actually, the possible existence of coordinated H_3 in the open structure (the existence of closed, triangular H_3^+ in the gas phase is well established)[56] has been suggested on theoretical grounds by Burdett et al.[57] On experimental grounds, Crabtree and Luo have proposed the formation of an open η^3-H_3 complex either as an intermediate or as a transition state to explain the exchange of dihydrogen and terminal hydride ligands at Re in $[ReH_2(\eta^2\text{-}H_2)(CO)(PMe_2Ph)_3]^+$.[8] More recently, we have interpreted the fluxionality in solution of $[(PP_3)Fe(H)(\eta^2\text{-}H_2)]^+$ [9,10] and $[(PP_3)Ru(H)(\eta^2\text{-}H_2)]^+$ [11] as involving a trihydrogen intermediate. Within this context, the isolation and characterization of **4** and **5** is thought-provoking as it might open a way to the synthesis of stable η^3-H_3 complexes through the design of appropriate metal fragments.

Acknowledgment. We thank "Progetti Finalizzati-Chimica Fine II", CNR, Rome, for supporting this work.

Supplementary Material Available: Tables of experimental and crystallographic data per **4**·THF (Table S1), anisotropic displacement parameters (Table S2), bond distances and angles (Tables S3 and S4, respectively), and torsion angles (Table S5) (16 pages). Ordering information is given on any current masthead page.

(53) Wang, H. H.; Pignolet, L. H. *Inorg. Chem.* **1980**, *19*, 1470.
(54) Braunstein, P.; Gomes Carnero, T. M.; Matt, D.; Tiripicchio, A.; Tiripicchio Camellini, M. *Angew. Chem., Int. Ed. Engl.* **1986**, *25*, 748.
(55) (a) Heinekey, D. M.; Millar, J. M.; Koetzle, T. F.; Payne, N. G.; Zilm, K. W. *J. Am. Chem. Soc.* **1990**, *112*, 909. (b) Zilm, K. W.; Heinekey, D. M.; Millar, J. M.; Payne, N. G.; Neshyba, S. P.; Duchamp, J. C.; Szczyrba, J. *J. Am. Chem. Soc.* **1990**, *112*, 920. (c) Heinekey, D. M.; Payne, N. G.; Sofield, C. D. *Organometallics* **1990**, *9*, 2643.
(56) Oka, T. *Phys. Rev. Lett.* **1980**, *45*, 531.
(57) Burdett, J. K.; Phillips, J. R.; Pourian, M. R.; Poliakoff, M.; Turner, J. J.; Upmacis, R. *Inorg. Chem.* **1987**, *26*, 3054.